

Use of Perfluorinated Phosphines to Provide Thermomorphing Anticancer Complexes for Heat-Based Tumor Targeting

Anna K. Renfrew, Rosario Scopelliti, and Paul J. Dyson*

Institut des Sciences et Ingénierie Chimiques, Ecole Polytechnique Fédérale de Lausanne (EPFL), CH-1015 Lausanne, Switzerland

Received October 15, 2009

A series of compounds of general formula $[\text{Ru}(\eta^6\text{-arene})(\text{pta})(\text{PR}_3)\text{Cl}]\text{BF}_4$ (arene = *p*-cymene or 4-phenyl-2-butanol; pta = 1,3,5-triaza-7-phosphatricyclo[3.3.1.1]decane, $\text{PR}_3 = \text{PPh}_2(p\text{-C}_6\text{H}_4\text{C}_2\text{H}_4\text{C}_8\text{F}_{17})$, $\text{PPh}(p\text{-C}_6\text{H}_4\text{C}_2\text{H}_4\text{C}_8\text{F}_{17})_2$, $\text{P}(p\text{-C}_6\text{H}_4\text{C}_2\text{H}_4\text{C}_8\text{F}_{17})_3$, PPh_3 or $\text{P}(p\text{-C}_6\text{H}_4\text{F})_3$) have been prepared and characterized by spectroscopic methods. The structure of $[\text{Ru}(\eta^6\text{-}p\text{-cymene})(\text{pta})\text{Cl}(\text{P}(p\text{-C}_6\text{H}_4\text{F})_3)]\text{BF}_4$ has also been established in the solid state by X-ray crystallography. The cytotoxicities of the compounds were determined in the A2780 and A2780 cisplatin-resistant cell lines revealing that the fluorinated phosphines significantly increase antiproliferative activity relative to their bis-chloride precursors. Two of the complexes were found to be thermoresponsive, that is, showing poor water solubility at 37 °C and good solubility at 42 °C, the temperature of a heated tumor, providing a method of tumor targeting. Incubation at 42 °C for 2 h resulted in improved cytotoxicities for two of the complexes.

Introduction

One of the main goals in the field of inorganic (or organometallic) antitumor drugs is to overcome the two major limitations of cisplatin, namely, poor selectivity and a high incidence of drug resistance. From the many metal-based drugs that have been developed, ruthenium has emerged as an attractive alternative to platinum because of its excellent activity in tumors where cisplatin is of limited use and because of its low general toxicity.^{1,2} Two ruthenium(III)

based drugs, KP1019³ and NAMI-A,⁴ have currently completed phase I clinical trials and are in, or set to enter, phase II trials. Both complexes behave quite differently to cisplatin in vivo; NAMI-A has been shown to be a strong inhibitor of metastasis while having little effect on primary tumors,⁵ whereas KP1019 effectively reduces colorectal tumors where cisplatin shows limited activity.⁶

Organometallic compounds are also attracting attention as anticancer drugs.⁷ In this context organoruthenium(II) compounds are promising,⁸ following recent studies that show they can react with biologically relevant targets.⁹ We have been developing a series of organometallic ruthenium (RAPTA) compounds (Chart 1) with an η^6 -arene ligand, a monodentate 1,3,5-triaza-7-phosphatricyclo[3.3.1.1]decane (pta) ligand and, in most cases, two labile chloride ligands (Figure 1). These compounds tend to exhibit low general toxicity in vivo, and depending on the particular compound and tumor model, are active against metastatic¹⁰ and primary tumors.¹¹

*To whom correspondence should be addressed. E-mail: paul.dyson@epfl.ch.

- (1) Clarke, M. J.; Zhu, F.; Frasca, D. R. *Chem. Rev.* **1999**, *99*, 2511.
- (2) Dyson, P. J.; Sava, G. *Dalton Trans.* **2006**, 1929.
- (3) (a) Smith, C. A.; Sutherland-Smith, A. J.; Keppler, B. K.; Kratz, F.; Baker, E. N. *J. Bio. Inorg. Chem.* **1996**, *1*, 424. (b) Hartinger, C. G.; Jakupec, M. A.; Zorbas-Seifried, S.; Groessl, M.; Egger, A.; Berger, W.; Zorbas, H.; Dyson, P. J.; Keppler, B. K. *Chem. Biodiversity* **2008**, *5*, 2140.
- (4) Alessio, E.; Mestroni, G.; Bergamo, A.; Sava, G. *Met. Ions Biol. Syst.* **2004**, *42*, 323.
- (5) Alessio, E.; Mestroni, G.; Bergamo, A.; Sava, G. *Curr. Top. Med. Chem.* **2004**, *4*, 1525.
- (6) Hartinger, C. G.; Zorbas-Seifried, S.; Jakuped, M. A.; Kynast, B.; Zorbas, H.; Keppler, B. K. *J. Inorg. Biochem.* **2006**, *100*, 891.
- (7) For example see: (a) Nguyen, A.; Top, S.; Pigeon, P.; Vèssieres, A.; Hillard, E. A.; Plamont, M.; Huche, M.; Rigamonti, C.; Jaouen, G. *Chem.—Eur. J.* **2009**, *15*, 684. (b) Top, S.; Thibaudeau, C.; Vèssieres, A.; Brule, E.; Le Bideau, F.; Joerger, J.; Plamont, M.; Samreth, S.; Edgar, A.; Marrot, J.; Herson, P.; Jaouen, G. *Organometallics* **2009**, *28*, 1414. (c) Strohfeldt, K.; Tacke, M. *Chem. Soc. Rev.* **2008**, *37*, 1174. (d) Hogan, M.; Claffey, J.; Pampillon, C.; Tacke, M. *Med. Chem.* **2008**, *4*, 91. (e) Kirin, S. I.; Ott, I.; Gust, R.; Mier, W.; Weyhermüller, T.; Metzler-Nolte, N. *Angew. Chem.* **2008**, *47*, 955. (f) Gross, A.; Metzler-Nolte, N. *J. Organomet. Chem.* **2009**, *694*, 1185. (g) Zobi, F.; Blacque, O.; Sigel, R. K. O.; Alberto, R. *Inorg. Chem.* **2007**, *46*, 10458. (h) Xavier, C.; Giannini, C.; Dall'Angelo, S.; Gano, L.; Maiorana, S.; Alberto, R.; Santos, I. *J. Bio. Inorg. Chem.* **2008**, *13*, 1335. (i) Hartinger, C. G.; Dyson, P. J. *Chem. Soc. Rev.* **2009**, *38*, 391.

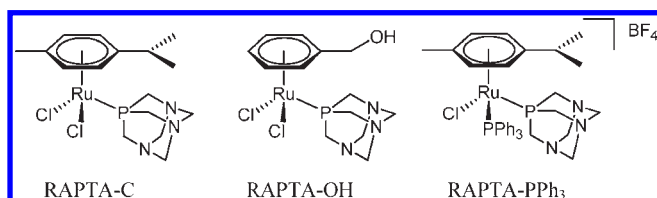
- (8) (a) Romerosa, A.; Saoud, M.; Campos-Malpartida, T.; Lidrissi, C.; Serrano-Ruiz, M.; Peruzzini, M.; Garrido, J. A.; Garcia-Maroto, F. *Eur. J. Inorg. Chem.* **2007**, 2803. (b) Schmid, W. F.; John, R. O.; Arion, V. B.; Jakupec, M. A.; Keppler, B. K. *Organometallics* **2007**, *26*, 6643. (c) Habtemariam, A.; Melchart, M.; Fernandez, R.; Parsons, S.; Oswald, I. D. H.; Parkin, A.; Fabbiani, F. P. A.; Davidson, J. E.; Dawson, A.; Aird, R. E.; Jodrell, D. I.; Sadler, P. J. *J. Med. Chem.* **2006**, *49*, 6858.

- (9) (a) Fish, R. H. *Coord. Chem. Rev.* **1999**, *185–186*, 569. (b) Chen, H.; Maestre, M. F.; Fish, R. H. *J. Am. Chem. Soc.* **1995**, *117*, 3631.

- (10) Scolaro, C.; Bergamo, A.; Brescacin, L.; Delfino, R.; Cocchietto, M.; Laurency, G.; Geldbach, T. J.; Sava, G.; Dyson, P. J. *J. Med. Chem.* **2005**, *48*, 4161.

- (11) Chatterjee, S.; Kundu, S.; Bhattacharyya, A.; Hartinger, C. G.; Dyson, P. J. *J. Biol. Inorg. Chem.* **2008**, *13*, 1149.

Chart 1. Examples of RAPTA-Type Compounds



The nature of the ligand sphere greatly influences the *in vitro* activity of the complexes. Increasing hydrophilicity through hydrogen bonding substituents on the arene ligand was shown to reduce both cellular uptake and cytotoxicity.¹² Accordingly, the replacement of a chloride ligand with hydrophobic PPh₃ was found to increase cellular uptake and consequently cytotoxicity, but also resulted in increased toxicity toward a non-tumorigenic cell line,¹³ which in turn could be linked to an increased reactivity toward DNA and a decrease in protein affinity. In related work, Romerosa et al. demonstrated that binding of [Ru(η^5 -C₅Me₃)(pta)Cl₂] to supercoiled DNA is greatly increased on replacement of the pta ligand by triphenylphosphine or triphenylphosphine monosulfonate,^{14,15} and a similar effect has been reported for Pt complexes,¹⁶ although the influence on general toxicity and protein binding was not investigated.

While the increase in cell uptake and consequently in cytotoxicity shown by the PPh₃-derivatized compounds is promising, it would be necessary to improve selectivity to reduce potential damage to healthy cells. A number of strategies have been employed in the design of metal-based drugs aimed at producing a complex which is preferentially active in the tumor environment;^{17,18} here we investigate the possibility of introducing selectivity through temperature-controlled solubility.

Thermotherapy is a treatment in which a heat source is applied to the tumor area causing an increase in temperature. The compact, disordered structure of tumor cells makes them less effective at dissipating heat than healthy cells and as result, the cells become weakened and more sensitive to chemotherapy.¹⁹ A number of chemotherapeutic agents have been tested in conjunction with thermotherapy, both *in vitro* and *in vivo*, and the results found to vary greatly between compounds.²⁰ While hyperthermia leads to additive

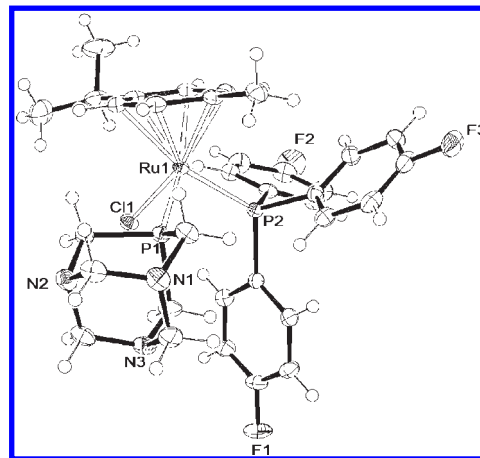


Figure 1. ORTEP representation of **8b**. Ellipsoids are drawn at the 50% probability level and the BF₄⁻ counteranion has been omitted for clarity. Key bond lengths (Å) and angles (deg) include: Ru1–Cl1 2.3819(6), Ru1–Cl1 2.3165(6), Ru1–P2 2.3424(6), Ru1–C_{avg} 2.26(2), Cl1–Ru1–P1 82.19, Cl1–Ru1–P2 87.94(2), P1–Ru1–P2 95.43(2).

cytotoxicity when used with oxaliplatin or nucleoside analogue gemcitabine, no interaction occurs with 5-fluorouracil or taxane.²¹ In contrast, a synergistic effect is observed when the treatment is applied with cisplatin, carboplatin, or alkylating agents such as cyclophosphamide and mephalan, with the degree of synergism increasing as the cell temperature is raised from 40.5–43.5 °C, although these compounds were not designed to be thermoresponsive.²¹ The reason for this effect is not clearly understood, but for cisplatin it is proposed to be due to increased DNA platination.¹⁹ Exploiting the difference in temperature between a tumor cell and healthy cell, a number of specifically designed thermoresponsive macromolecules have been investigated for application with thermotherapy. Several types of liposomes have been developed for the release of chemotherapeutic agents at the heated tumor temperature,²² and doxorubicin containing liposomes have entered clinical trials.²³ In a different strategy, certain peptides or proteins become hydrophobic above 40 °C and aggregate in the heated tumor cells, allowing increased accumulation of a conjugated drug.²⁴

Phosphines functionalized with perfluorinated chains are known for their thermomorphic properties with a significant increase in solubility observed on raising the temperature.²⁵ With the aim of developing thermomorphic complexes, that is, complexes that show increased solubility at a heated tumor, a series of RAPTA-type compounds were prepared that incorporate fluorophosphine ligands. As far as we are aware these compounds represent the first examples of thermomorphic small molecule-based drugs.

(12) Scolaro, C.; Geldbach, T. J.; Rochat, S.; Dorcier, A.; Gossens, C.; Bergamo, A.; Cocchietto, M.; Tavernelli, I.; Sava, G.; Rothlisberger, U.; Dyson, P. J. *Organometallics* **2006**, *25*, 756.

(13) Scolaro, C.; Chaplin, A. B.; Hartinger, C. G.; Bergamo, A.; Cocchietto, M.; Keppler, B. K.; Sava, G.; Dyson, P. J. *Dalton Trans.* **2007**, 5065.

(14) Romerosa, A.; Campos-Malpartida, T.; Lidrissi, C.; Saoud, M.; Serrano-Ruiz, M.; Peruzzini, M.; Garrido-Cardenas, J. A.; Garcia-Maroto, F. *Inorg. Chem.* **2006**, *45*, 1289.

(15) Romerosa, A.; Saoud, M.; Campos-Malpartida, T.; Lidrissi, C.; Serrano-Ruiz, M.; Peruzzini, M.; Garrido-Cardenas, J. A.; Garcia-Maroto, F. *Eur. J. Inorg. Chem.* **2007**, *18*, 2803.

(16) (a) McCaffrey, L. J.; Henderson, W.; Nicholson, B. K.; Mackay, J. E.; Dinger, M. B. *Dalton Trans.* **1997**, 2577. (b) McCaffrey, L. J.; Henderson, W.; Nicholson, B. K. *Dalton Trans.* **2000**, 2753.

(17) (a) Kelland, L. R.; Abel, G.; McKeage, M. J.; Jones, M.; Goddard, P. M.; Valenti, M.; Murrer, B. A.; Harrap, K. R. *Cancer Res.* **1993**, *53*, 2581. (b) Failes, T. W.; Cullinane, C.; Diakos, C. I.; Yamamoto, N.; Lyons, J. G.; Hambley, T. W. *Chem.—Eur. J.* **2007**, *13*, 2974.

(18) Galanski, M.; Baumgartner, C.; Meelich, K.; Arion, V. B.; Fremuth, M.; Jakupec, M. A.; Schluga, P.; Hartinger, C. G.; von Keyserlingk, N. G.; Keppler, B. K. *Inorg. Chim. Acta* **2004**, *357*, 3237.

(19) Gabano, E.; Colangelo, D.; Ghezzi, A. R.; Osella, D. *J. Inorg. Biochem.* **2008**, *102*, 629.

(20) Issels, R. D. *Eur. J. Cancer* **2008**, *44*, 2546.

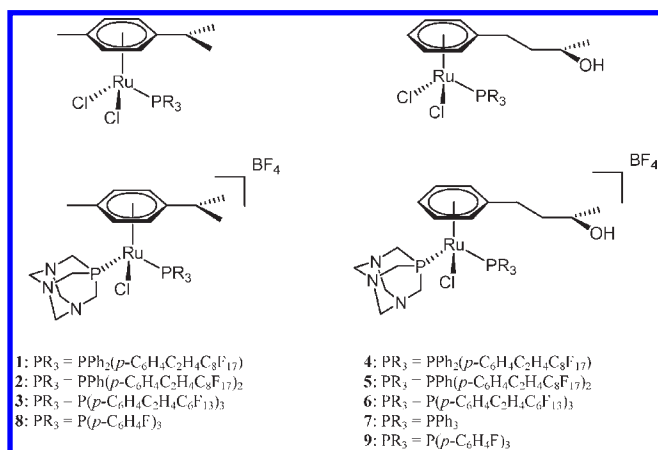
(21) Urano, M.; Kuroda, M.; Nishimura, Y. *Int. J. Hyperthermia* **1999**, *15*, 79.

(22) (a) Needham, D.; Anyarambatla, G.; Kong, G.; Dewhirst, M. W. *Cancer Res.* **2000**, *60*, 1197. (b) Lindner, L. H.; Eichhorn, M. E.; Eibl, H.; Teichert, N.; Schmitt-Sody, M.; Issels, R. D.; Dellian, M. *Clin. Cancer Res.* **2004**, *10*, 2168.

(23) Jones, E.; Vujaskovic, Z.; Dewhirst, M.; Craciunescu, O.; Stauffer, P.; Prosnitz, L.; Kimmick, G.; Blackwell, K. (Abstract) In: *10th international congress of hyperthermic oncology*, Munich, Germany, 2008.

(24) (a) Furgeon, D. Y.; Dreher, M. R.; Chilkoti, A. *J. Controlled Release* **2006**, *110*, 362. (b) Wagner, E. *Expert Opin. Biol. Ther.* **2007**, *7*, 587.

(25) (a) Soos, T.; Bennett, B. L.; Rutherford, D.; Barthel-Rosa, L. P.; Gladysz, J. A. *Organometallics* **2001**, *20*, 3079. (b) Wende, M.; Gladysz, J. A. *J. Am. Chem. Soc.* **2003**, *125*, 5861.

Chart 2. Structures of Compounds **1a–9a** (top) and **1b–9b** (bottom)

Results and Discussion

Ruthenium(II)-arene complexes with fluorophosphine ligands **1–6**, **8**, and **9** (Chart 2) were prepared using the two-step process shown in Scheme 1. Reaction of the appropriate dimers, $[\text{Ru}(\eta^6\text{-}p\text{-cymene})\text{Cl}_2]_2$ or $[\text{Ru}(\eta^6\text{-}4\text{-phenyl-2-butanol})\text{Cl}_2]_2$, with a stoichiometric amount of the fluorophosphine ligands, PR_3 , affords the dichloride complexes $[\text{Ru}(\eta^6\text{-arene})(\text{PR}_3)_2\text{Cl}_2]$ **1a–5a**, **8a**, and **9a** in good yield. Subsequent reaction of **1a–5a** with an excess of NH_4BF_4 , followed by dropwise addition of the amphiphilic phosphine pta, results in the formation of the monocationic complexes $[\text{Ru}(\eta^6\text{-arene})(\text{pta})(\text{PR}_3)\text{Cl}]\text{BF}_4$ **1b–5b**. Addition of pta followed by the fluorophosphine is also possible, but the yield of the final product is considerably lower. All complexes show good solubility in fluorobenzene and chlorinated solvents and moderate solubility in polar solvents. Complexes **1b–3b** are insoluble in water, whereas the 4-phenyl-2-butanol analogues **4b** and **5b** are more soluble in polar solvents, and **4b** is also water-soluble. To evaluate the influence of the fluororous chain on solubility, complexes $[\text{Ru}(\eta^6\text{-}4\text{-phenyl-2-butanol})(\text{pta})(\text{PPh}_3)\text{Cl}]\text{BF}_4$ **7b**, $[\text{Ru}(\eta^6\text{-}p\text{-cymene})(\text{pta})(\text{P}(\text{C}_6\text{H}_4\text{F}_3)_3)\text{Cl}]\text{BF}_4$ **8b**, and $[\text{Ru}(\eta^6\text{-}4\text{-phenyl-2-butanol})(\text{pta})(\text{P}(\text{C}_6\text{H}_4\text{F}_3)_3)\text{Cl}]\text{BF}_4$ **9b** were prepared for comparison purposes. All compounds are soluble in chlorinated and polar solvents, and **7b** and **9b** are also water-soluble. Compounds with the *p*-cymene ligand, that is, **1b–3b** and **8b**, are obtained as enantiomers that are indistinguishable by NMR spectroscopy. Compounds containing the chiral 4-phenyl-2-butanol ligand, **4b–7b** and **9b**, were obtained as two diastereoisomers that give rise to two sets of peaks in the ^{31}P NMR spectra in CDCl_3 , and the isomers were not separated and were evaluated as a mixture.

All compounds were characterized by ^1H and ^{31}P NMR spectroscopy and electrospray ionization mass spectrometry (ESI-MS). Table 1 lists the ^{31}P NMR spectroscopic data of **1a–5a** and **7a–9a** in CDCl_3 , each of which exhibits a singlet due to the fluorophosphine ligand. As expected, compounds **1b–9b**, that contain a fluorophosphine (or PPh_3 in the case of **7b**) and pta ligand, display two characteristic doublets resulting from coupling between the two ^{31}P nuclei. In the case of **4b–7b** and **9b**, two diastereoisomers are present in the ^{31}P NMR spectra as two sets of doublets at a ratio of approximately 1:1, Table 1 describes both isomers. The number and size of the electron-withdrawing fluororous chains on the phosphine ligand has little influence on the chemical

shift presumably because of the insulation provided by the ethylene spacer.

Structural Characterization of 8b in the Solid State. Single crystals of **8b** suitable for X-ray diffraction were obtained via slow diffusion (see Experimental Section for details), and the resulting X-ray structure is shown in Figure 1. The ruthenium(II) compound exhibits the piano-stool geometry typical of half-sandwich complexes and is very similar to that of $[\text{Ru}(\eta^6\text{-cymene})(\text{pta})(\text{PPh}_3)\text{Cl}]\text{BF}_4$, although the $\text{Ru}-\text{P}(\text{C}_6\text{H}_4\text{F}_3)_3$ bond length is slightly shorter [2.3424(6) vs 2.3590(14) Å].¹³ Otherwise, the Ru -arene, $\text{Ru}-\text{Cl}$, and Ru -pta bond lengths and angles are similar to those of RAPTA-C²⁶ and other RAPTA derivatives.²⁷

Behavior in Aqueous Solution. The hydrolysis of the water-soluble compound, that is, **4b**, was studied by ^{31}P NMR spectroscopy. Hydrolytic decomposition is central to the mode of action of cisplatin and is also thought to be relevant for mono and dichloro ruthenium(II)-arene based drugs which undergo rapid hydrolysis in water containing 5 mM NaCl (the approximate salt concentration inside a cell).²⁸ Hydrolysis is reversed by addition of 100 mM NaCl (corresponding to the salt concentration of blood plasma). Hydrolysis of RAPTA compounds with two Cl-ligands occurs readily with the major species formed being $[\text{Ru}(\eta^6\text{-arene})(\text{pta})\text{Cl}(\text{H}_2\text{O})]^+$. In D_2O the ^{31}P NMR spectrum of **4b** displays two doublets at 31.9 and -43.7 ppm corresponding to the fluororous phosphine and pta ligands, respectively. However, following about 5 h of incubation at 37 °C, two new doublets are also present at 30.4 and -41.2 and are thought to represent the hydrolysis product, $[\text{Ru}(\eta^6\text{-}4\text{-phenyl-2-butanol})(\text{H}_2\text{O})(\text{pta})(\text{PPh}_2(p\text{-C}_6\text{H}_4\text{C}_2\text{H}_4\text{C}_8\text{F}_{17}))_2]^+$. The new peaks disappear on addition of 100 mM NaCl, and no further change is observed following 7 days of incubation.

The solubility of phosphines with fluororous alkyl chains is known to have a strong dependence on temperature. Gladysz et al. reported a 600-fold increase in the solubility of $\text{P}(\text{C}_2\text{H}_4\text{C}_8\text{F}_{17})_3$ in octane as the temperature changes from -20 to 80 °C.²⁵ The solubility of **1b–9b** in water was measured over the temperature range 20 – 45 °C (Figure 2) with **2b**, **3b**, **6b**, and **8b** being insoluble across the entire temperature range (see Experimental Section for details).

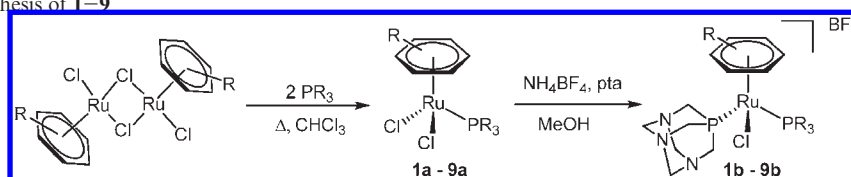
Complexes **4b**, **7b**, and **9b** show moderate solubility at room temperature (2.5–5 mM), and while the solubility of **7b** and **9b** changes only slightly over the temperature range, the solubility of **4b** increases by approximately an order of magnitude on raising the temperature by 25 °C. At 37 °C **4b** is already soluble to a concentration 3 orders of magnitude greater than its IC_{50} concentration (see below), limiting its potential for heat-based tumor targeting. In contrast, **1b** and **5b**, which are scarcely soluble at

(26) Allardyce, C. S.; Dyson, P. J.; Ellis, D. J.; Heath, S. L. *Chem. Commun.* **2001**, 1396.

(27) (a) Ang, W. H.; Parker, L. J.; De Luca, A.; Juillerat-Jeanneret, L.; Morton, C. J.; Lo Bello, M.; Parker, M. W.; Dyson, P. J. *Angew. Chem., Int. Ed.* **2009**, *48*, 3854–3857. (b) Casini, A.; Gabbiani, C.; Sorrentino, F.; Rigobello, M. P.; Bindoli, A.; Geldbach, T. J.; Marrone, A.; Re, Nazzareno, N.; Hartinger, C. G.; Dyson, P. J.; Messori, L. *J. Med. Chem.* **2008**, *51*, 6773. (c) Dorcier, A.; Ang, W. H.; Bolano, S.; Gonsalvi, L.; Juillerat-Jeanneret, L.; Laurenczy, G.; Peruzzini, M.; Phillips, A. D.; Zanobini, F.; Dyson, P. J. *Organometallics* **2006**, *25*, 4090.

(28) (a) Wang, F.; Chen, H.; Parsons, S.; Oswald, I. D. H.; Davidson, J. E.; Sadler, P. J. *Chem.—Eur. J.* **2003**, *9*, 5810. (b) Scolaro, C.; Hartinger, C. G.; Allardyce, C. S.; Keppler, B. K.; Dyson, P. J. *J. Inorg. Biochem.* **2008**, *102*, 1743.

Scheme 1. General Synthesis of 1–9

Table 1. ^{31}P NMR Data for 1–9 in CDCl_3

complex	$\delta^{31}\text{P}$ (PR_3)	$\delta^{31}\text{P}$ (pta)
1a	24.2	
2a	23.6	
3a	23.6	
4a	28.0	
5a	27.3	
7a	27.7	
8a	23.0	
9a	24.6	
1b	30.0 ($^2J_{\text{PP}} = 52$ Hz)	-42.7 ($^2J_{\text{PP}} = 54$ Hz)
2b	29.7 ($^2J_{\text{PP}} = 55$ Hz)	-43.1 ($^2J_{\text{PP}} = 55$ Hz)
3b	29.8 ($^2J_{\text{PP}} = 55$ Hz)	-43.3 ($^2J_{\text{PP}} = 55$ Hz)
4b	31.3 ($^2J_{\text{PP}} = 54$ Hz)	-40.4 ($^2J_{\text{PP}} = 55$ Hz)
5b	31.4 ($^2J_{\text{PP}} = 54$ Hz)	-40.5 ($^2J_{\text{PP}} = 54$ Hz)
6b ^a	30.8 ($^2J_{\text{PP}} = 53$ Hz)	-41.4 ($^2J_{\text{PP}} = 54$ Hz)
	30.9 ($^2J_{\text{PP}} = 54$ Hz)	-41.5 ($^2J_{\text{PP}} = 54$ Hz)
	29.2 ($^2J_{\text{PP}} = 54$ Hz)	-42.0 ($^2J_{\text{PP}} = 54$ Hz)
	29.4 ($^2J_{\text{PP}} = 54$ Hz)	-42.2 ($^2J_{\text{PP}} = 55$ Hz)
7b	30.4 ($^2J_{\text{PP}} = 53$ Hz)	-42.5 ($^2J_{\text{PP}} = 54$ Hz)
	30.5 ($^2J_{\text{PP}} = 53$ Hz)	-42.7 ($^2J_{\text{PP}} = 54$ Hz)
8b	28.8 ($^2J_{\text{PP}} = 54$ Hz)	-42.5 ($^2J_{\text{PP}} = 54$ Hz)
9b	30.3 ($^2J_{\text{PP}} = 54$ Hz)	-41.0 ($^2J_{\text{PP}} = 54$ Hz)
	30.5 ($^2J_{\text{PP}} = 53$ Hz)	-41.2 ($^2J_{\text{PP}} = 54$ Hz)

^a Recorded in d^6 -DMSO.

37 °C (40–80 μM), show a 4-fold increase in solubility at 42 °C, and therefore represent much better candidates for thermal chemotherapy.

In Vitro Anticancer Activity at 37 °C. The in vitro cytotoxicity of the compounds was evaluated using the MTT assay which estimates mitochondrial dehydrogenase activity as an indication of cell viability. The compounds were incubated at various concentrations in the ovarian cancer cell line A2780 and the cisplatin-resistant variant, A2780cisR, and cell viability measured after 72 h incubation. Each experiment was performed in triplicate, repeated twice, and the IC_{50} values listed in Table 2 were calculated as an average over the two experiments. Because of the poor aqueous solubility, compounds were added to medium as DMSO solutions, to give a final concentration of 0.5% DMSO. Reliable IC_{50} values could not be obtained for compounds 2a, 3a, 3b, and 6b as the complexes formed an oil or precipitated when added to the cell medium.

Related ruthenium(II)-arene-pta compounds investigated for in vitro activity are generally found to have low antiproliferative activity in vitro, but nevertheless display excellent in vivo activities, with the pta ligand being fundamental to the cytotoxic effect.^{10,11,29} The IC_{50} values of the new RAPTA complexes with fluorophosphine ligands are consistently lower than those of the dichloro-pta complexes, being up to 2 orders of magnitude more active. Interestingly, the pta ligand has little effect on cytotoxicity with the activity of pta

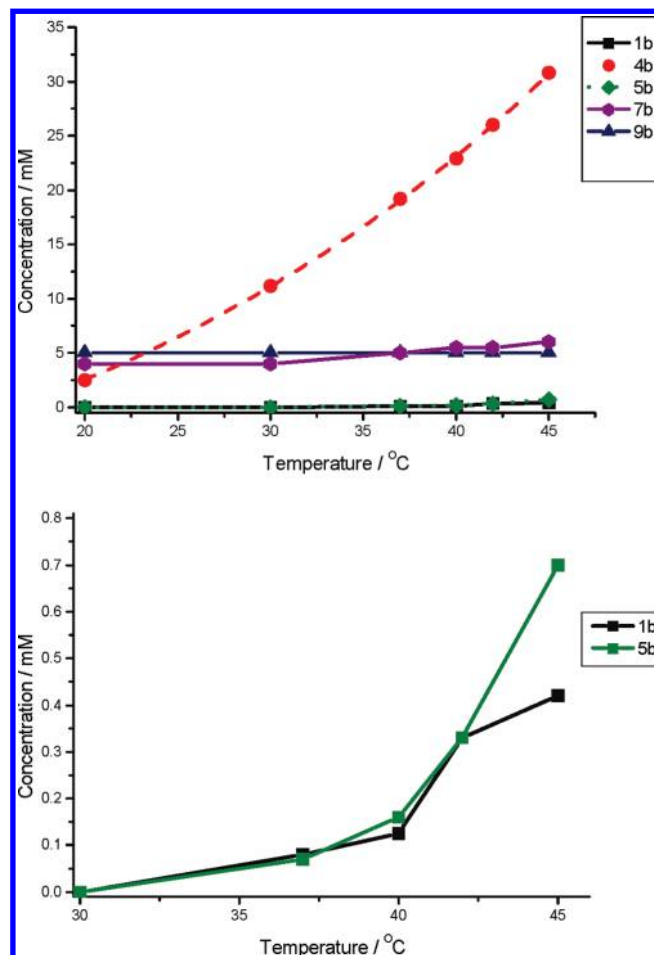


Figure 2. (top) Water solubility of the (sparingly) soluble complexes as a function of temperature; plot of 4b fitted to $y = y_0 + Ae^{x/b}$. (bottom) Water solubility of thermomorphic complexes 1b and 5b as a function of temperature.

complexes 1b–9b being very close to that of the analogous dichloro complexes 1a–9a. The nature of the fluorophosphine ligand, however, appears to have a considerable influence on the in vitro activity. While the cytotoxicity of 7b is relatively low (IC_{50} in A2780 = 184 μM), the analogous mono fluorous-chain complex, 4b shows very good activity (IC_{50} in A2780 = 6 μM). It seems unlikely that the cytotoxic effect is due to release of the fluorophosphine ligand as NMR spectroscopy indicates that the ligand remains coordinated to the ruthenium center even after 1 week in solution, and moreover, the free ligand was found to be completely inactive. As the fluorous chain has little electronic effect at the metal, it is probable that the increase in cytotoxicity is due to improved uptake resulting from the hydrophobic fluorophosphine ligand.

Compound 1b is the most active of the series, with a cytotoxicity equivalent to cisplatin in the A2780 cells and

(29) Bergamo, A.; Masi, A.; Dyson, P. J.; Sava, G. *Int. J. Oncol.* **2008**, *33*, 1281.

Table 2. IC₅₀ Values of the Complexes Determined in the A2780 and A2780cisR Cell Lines

compound	A2780/ μ M	A2780cisR/ μ M
PPh ₂ (C ₆ H ₄ C ₂ H ₄ C ₈ F ₁₇)	> 400	> 400
1a	16 ± 2	25 ± 2
4a	6 ± 0.5	11 ± 2
5a	> 200	> 200
8a	77 ± 2	> 200
9a	63 ± 5	118 ± 7
1b	1.5 ± 0.3	5 ± 0.5
2b	87 ± 6	108 ± 3
4b	6 ± 1.5	13 ± 1
5b	97 ± 18	> 200
7b	184 ± 12	> 200
8b	73 ± 2	172 ± 6
9b	41 ± 4	78 ± 3

a superior cytotoxicity in the resistant cell line.³⁰ To exclude the possibility of a DMSO effect, **4b** was tested in both pure medium and a DMSO solution but negligible difference was found between the resulting values. Typically, IC₅₀ values determined for the cisplatin resistant line are about 2-fold higher than for the standard A2780 cells. By comparison, cisplatin is around 20 times less active in the resistant line.³⁰ Cisplatin resistance in A2780cisR cells has been attributed to reduced uptake into the cell,³¹ increased DNA repair,³² and increased levels of glutathione transferases and other detoxification proteins,³³ which implies that the mode of uptake and action of these ruthenium(II)-arene compounds is markedly different to that of cisplatin.

In Vitro Activity at 42 °C. The in vitro activities of compounds **1b**, **4b**, and **5b** (having shown temperature dependent solubility in water) were further studied in the absence of DMSO at 37 and 42 °C. According to an established procedure,¹⁹ the cells were incubated with various concentrations of the compounds at 42 °C for 2 h, then for a further 72 h at 37 °C. Under these conditions, negligible reduction of cell viability between standard and heated cells was observed in control experiments (without the addition of a compound). In both the A2780 and cisplatin resistant line, **1b** and **4b** show an increase in cytotoxicity following the procedure that includes the 2 h exposure to a temperature of 42 °C (Table 3). Compound **1b** proved to be more active following 2 h exposure at 42 °C in both cell lines. The difference in A2780 cells was less marked for **4b**, though still significant in the resistant cell line. The high IC₅₀ value of **5b** in the dilution including DMSO (97 μ M, see Table 1) made it impossible to prepare an aqueous solution or even a suspension at a relevant concentration, and therefore reliable IC₅₀ values could not be obtained.

The greater cytotoxicity of **1b** and **4b** at elevated temperatures is likely to be due to their increased solubility at the higher temperature, facilitating availability within the cell medium and ultimately within the cell itself following uptake. However, at this stage it would be unwise to rule out other phenomena for the observed

Table 3. IC₅₀ Values in μ M of Complexes Determined in the A2780 (above) and A2780cisR Cell Lines (below) at 37 and 42 °C

compound	A2780 (37 °C)	A2780 (42 °C)
1b	3 ± 0.2	2 ± 0.3
4b	11 ± 2	9 ± 1

compound	A2780cisR (37 °C)	A2780cisR (42 °C)
1b	3 ± 0.2	2 ± 0.3
4b	14 ± 3	9 ± 1.5

trend. It is noteworthy that the incorporation of fluoro-phosphine ligands in combination with an amphiphilic phosphine (pta) into the ruthenium(II)-arene moiety tends to increase antiproliferative activity in the A2780 and A2780cisR cell lines with respect to RAPTA-type compounds that contain pta alone. The temperature-dependent solubility of **1b** and **4b** in water (thermomorphic behavior) and modest temperature dependent in vitro activity, which provides a way of selectively targeting tumor tissue in vivo by the application of heat at the tumor site, is quite encouraging. Such a targeting method is currently undergoing evaluation using macromolecular thermomorphic materials. As far as we are aware, the compounds described herein represent the first examples deliberately designed of small molecules where such a strategy has been applied, although small molecule alkylating agents, including cisplatin, that do not possess thermoresponsive properties have been evaluated in thermotherapy.²¹ While it is likely that the ideal compound has yet to be prepared and evaluated, this approach could prove to be important in the design of future metal based drugs and potentially small organic molecules with thermomorphic properties. This novel approach also offers a new dimension to the use of fluorine-containing compounds in medicinal chemistry, where F-atoms or CF₃ groups are usually used to modify the metabolism of a drug.³⁴

Experimental Section

All manipulations were carried out using standard Schlenk techniques with all solvents degassed prior to use. The ruthenium dimers, [Ru(η^6 -cymene)Cl₂]₂ and [Ru(η^6 -4-phenyl-2-butanol)Cl₂]₂, pta, and **8a** were synthesized according to literature procedures.^{12,35–37} Fluorophosphine ligands were purchased from Fluorous Technologies (Pittsburgh, U.S.A.). ¹H and ³¹P NMR spectra were recorded on a Bruker Avance DPX spectrometer at room temperature. H_o, H_m, and H_p refer to aromatic protons *ortho*-H, *meta*-H, and *para*-H, respectively. ESI-MS of the complexes were obtained on a ThermoFinnigan LCQ Deca XP Plus quadrupole ion trap instrument set in positive mode (solvent: methanol; flow rate: 5 μ L/min; spray voltage: 5 kV; capillary temperature: 100 °C; capillary voltage: 20 V), as described previously.³⁸ Melting points were obtained on a Stuart Scientific SMP3 melting point apparatus.

Synthesis of [Ru(η^6 -*p*-cymene)Cl₂(PPh₂(*p*-C₆H₄C₂H₄C₈F₁₇))]
1a. [Ru(η^6 -*p*-cymene)Cl₂]₂ (100 mg, 0.18 mmol) and PPh₂(*p*-C₆H₄-C₂H₄C₈F₁₇) (260 mg, 0.36 mmol) were refluxed in chloroform

(30) Auzias, M.; Therrien, B.; Süß-Fink, G.; Štěpnička, P.; Ang, W. H.; Dyson, P. J. *Inorg. Chem.* **2008**, *47*, 578.

(31) Ohmichi, M.; Hayakawa, J.; Tasaka, K.; Kurachi, H.; Murata, Y. *Trends Pharmacol. Sci.* **2005**, *26*, 113.

(32) Masuda, H.; Ozols, R. F.; Lai, G.-M.; Fojo, A.; Rothenberg, M.; Hamilton, T. C. *Cancer Res.* **1988**, *48*, 5713.

(33) Safaei, R. *Cancer Lett.* **2006**, *234*, 34.

(34) Purser, S.; Moore, P. R.; Swallow, S.; Gouverneur, V. *Chem. Soc. Rev.* **2008**, 320.

(35) (a) Zelonka, R. A.; Baird, M. C. *Can. J. Chem.* **1972**, *50*, 3063. (b) Bennett, M. A.; Smith, A. K. *Dalton Trans.* **1974**, 233.

(36) Daigle, D. J.; Pepperman, A. B.; Vail, S. L. *J. Heterocycl. Chem.* **1974**, *11*, 407.

(37) Serron, S. A.; Nolan, S. P. *Organometallics* **1995**, *14*, 4611.

(38) Dyson, P. J.; McIndoe, J. S. *Inorg. Chim. Acta* **2003**, *354*, 68.

(50 mL) for 8 h. The solvent volume was reduced in vacuo to about 10 mL, and the product precipitated with hexane (10 mL). The resulting red powder was filtered and washed with hexane (2 × 20 mL). Yield; 244 mg (67%).

¹H NMR (CDCl₃): δ 7.79–7.81 (m, 6H, PPh₂Ar), 7.42–7.44 (m, 8H, PPh₂Ar), 5.22 (d, ³J_{HH} = 5.6 Hz, 2H, H_m), 5.03 (d, ³J_{HH} = 6.0 Hz, 2H, H_o), 2.96 (t, ³J_{HH} = 6.1 Hz, 2H, PhCH₂CH₂C₈F₁₇), 2.77–2.79 (m, 1H, ¹Pr), 2.40–2–48 (m, 2H, PhCH₂CH₂C₈F₁₇), 1.89, (s, 3H, arene-CH₃), 1.13 (d, ³J_{HH} = 6.5 Hz, 6H, CH(CH₃)₂). ³¹P NMR (CD₂Cl₂): δ 24.2 (s, PPh₂Ar). ESI-MS (acetone) *m/z* = 1036.2 [Ru(η⁶-*p*-cymene)Cl₂(PPh₂Ph(C₂H₄C₈F₁₇))Na⁺ (90%), *m/z* = 977.6 [Ru(η⁶-*p*-cymene)Cl(PPh₂(*p*-C₆H₄C₂H₄C₈F₁₇))] (75%), *m/z* = 725.1 [HOPPh₂(*p*-C₆H₄C₂H₄C₈F₁₇)]⁺ (100%).

Compounds **1a–5a** and **7a–9a** were prepared according to the procedure described for [Ru(η⁶-*p*-cymene)Cl₂(PPh₂(*p*-C₆H₄C₂H₄C₈F₁₇))] **1a**.

[Ru(η⁶-*p*-cymene)Cl₂(PPh(*p*-C₆H₄C₂H₄C₈F₁₇))₂] **2a**. [Ru(η⁶-*p*-cymene)Cl₂]₂ (52 mg, 0.09 mmol) and PPh(*p*-C₆H₄C₂H₄C₈F₁₇)₂ (213 mg, 0.18 mmol). Yield; 189 mg (72%). Red powder.

¹H NMR (CDCl₃): δ 7.76–7.80 (m, 6H, PPhAr₂), 7.43–7.45 (m, 7H, PPhAr₂), 5.22 (d, ³J_{HH} = 6.1 Hz, 2H, H_m), 5.05 (d, ³J_{HH} = 5.8 Hz, 2H, H_o), 2.98 (t, ³J_{HH} = 5.8 Hz, 4H, PhCH₂CH₂C₈F₁₇), 2.76–2–79 (m, 1H, ¹Pr), 2.41–2.50 (m, 4H, PhCH₂CH₂C₈F₁₇), 1.89 (s, 3H arene-CH₃), 1.12 (d, ³J_{HH} = 6.4 Hz, 6H, CH(CH₃)₂). ³¹P NMR (CD₂Cl₂): δ 23.6 (s, PPhAr₂). ESI-MS (acetone) *m/z* = 1482.0 [Ru(η⁶-*p*-cymene)Cl₂(PPh(*p*-C₆H₄C₂H₄C₈F₁₇))Na⁺ (60%), *m/z* = 1424.3 [Ru(η⁶-*p*-cymene)Cl(PPh(*p*-C₆H₄C₂H₄C₈F₁₇))] (70%), *m/z* = 1170.7 [HO(PPh(*p*-C₆H₄C₂H₄C₈F₁₇))] (100%).

[Ru(η⁶-*p*-cymene)Cl₂(P(*p*-C₆H₄C₂H₄C₆F₁₃))₃] **3a**. [Ru(η⁶-*p*-cymene)Cl₂]₂ (52 mg, 0.09 mmol) and P(*p*-C₆H₄C₂H₄C₆F₁₃)₃ (250 mg, 0.19 mmol). Yield; 223 mg (70%), red powder.

¹H NMR (CDCl₃): δ 7.76–7.80 (m, 6H, PAr₃), 7.43–7.45 (m, 6H, PAr₃), 5.22 (d, ³J_{HH} = 6.3 Hz, 2H, H_m), 5.05 (d, ³J_{HH} = 5.8 Hz, 2H, H_o), 2.99–3.03 (m, 6H, PhCH₂CH₂C₆F₁₃), 2.73–2–83 (m, 1H, ¹Pr), 2.46–2.49 (m, 6H, PhCH₂CH₂C₆F₁₃), 1.89 (s, 3H arene-CH₃), 1.12 (d, ³J_{HH} = 6.7 Hz, 6H, CH(CH₃)₂). ³¹P NMR (CD₂Cl₂): δ 23.6 (s, PAr₃). ESI-MS (acetone) *m/z* = 1482.0 [Ru(η⁶-*p*-cymene)Cl₂(P(*p*-C₆H₄C₆F₁₃))Na⁺ (60%), *m/z* = 1424.3 [Ru(η⁶-*p*-cymene)Cl(P(*p*-C₆H₄C₆F₁₃))] (70%), *m/z* = 1170.7 [HO(P(*p*-C₆H₄C₆F₁₃))] (100%).

[Ru(η⁶-4-phenyl-2-butanol)Cl₂(PPh₂(*p*-C₆H₄C₂H₄C₈F₁₇))] **4a**. [Ru(η⁶-4-phenyl-2-butanol)Cl₂]₂ (116 mg, 0.21 mmol) and PPh₂(*p*-C₆H₄C₂H₄C₈F₁₇) (304 mg, 0.43 mmol). Yield; 389 mg (92%), red powder.

¹H NMR (CDCl₃): δ 7.70–7.92 (m, 6H, PPh₂Ar), 7.28–7.44 (m, 8H, PPh₂Ar), 5.28, (br, 2H, H_m) 5.16 (d, ³J_{HH} = 5.6 Hz, 2H, H_o), 4.59 (m, 1H, H_p), 2.96–3.00 (m, 2H, PhCH₂CH₂C₈F₁₇), 2.74–2–77 (m, 1H, HCOH), 2.42–2–46 (m, 2H, PhCH₂CH₂C₈F₁₇), 1.94–1.98 (m, 2H arene-CH₂CH₂), 1.77–1.80 (m, 2H, arene-CH₂CH₂), 1.25 (d, ³J_{HH} = 6.2 Hz, 3H, CH₃). ³¹P NMR (CD₂Cl₂): δ 28.0 (s, PPh₂Ar). ESI-MS (acetone) *m/z* = 1052.4 [Ru(η⁶-4-phenyl-2-butanol)Cl₂(PPh₂(*p*-C₆H₄C₂H₄C₈F₁₇))Na⁺ (100%), *m/z* = 994.5 [Ru(η⁶-4-phenyl-2-butanol)Cl(PPh₂(*p*-C₆H₄C₂H₄C₈F₁₇))] (65%), *m/z* = 725.1 [HOPPh₂(*p*-C₆H₄C₂H₄C₈F₁₇))] (100%).

[Ru(η⁶-4-phenyl-2-butanol)Cl₂(PPh(*p*-C₆H₄C₂H₄C₈F₁₇))₂] **5a**. [Ru(η⁶-4-phenyl-2-butanol)Cl₂]₂ (144 mg, 0.27 mmol) and PPh(*p*-C₆H₄C₂H₄C₈F₁₇)₂ (617 mg, 0.54 mmol). Yield; 611 mg (88%), red powder.

¹H NMR (CDCl₃): δ 7.71–7.73 (m, 6H, PPhAr₂), 7.35–7.46 (m, 7H, PPhAr₂), 5.28, (d, ³J_{HH} = 5.5 Hz, 2H, H_m) 5.18 (d, 2H, ³J_{HH} = 5.8 Hz, H_o), 4.53 (m, 1H, H_p), 2.92–2.95 (m, 4H, PhCH₂CH₂C₈F₁₇), 2.81–2.84 (m, 1H, HCOH), 2.43–2.46 (m, 4H, PhCH₂CH₂C₈F₁₇), 1.94–1.97 (m, 2H arene-CH₂CH₂), 1.80–1.83 (m, 2H, arene-CH₂CH₂), 1.27 (d, ³J_{HH} = 6.5 Hz, 3H, CH₃). ³¹P NMR (CDCl₃): δ 27.3 (s, PPhAr₂). ESI-MS (acetone) *m/z* = 1499.0 [Ru(η⁶-4-phenyl-2-butanol)Cl₂(PPh(*p*-C₆H₄C₂H₄C₈F₁₇))Na⁺ (60%), *m/z* = 1441.3

[Ru(η⁶-4-phenyl-2-butanol)Cl(PPh(*p*-C₆H₄C₂H₄C₈F₁₇))₂]⁺ (70%), *m/z* = 1170.7 [HO(PPh(*p*-C₆H₄C₂H₄C₈F₁₇))] (100%).

[Ru(η⁶-4-phenyl-2-butanol)Cl₂(PPh₃)] **7a**. [Ru(η⁶-4-phenyl-2-butanol)Cl₂]₂ (100 mg, 0.16 mmol) and PPh₃ (84 mg, 0.32 mmol). Yield; 155 mg (83%), red powder.

¹H NMR (CDCl₃): δ 7.32–7.56 (m, 6H, PPh₃), 6.97–7.24 (m, 6H, PPh₃), 5.66 (d, ³J_{HH} = 5.0 Hz, 2H, H_m), 5.43 (d, ³J_{HH} = 3.6 Hz, 2H, H_o) 4.75 (d, 1H, H_p), 2.56–2.72 (m, 1H, HCOH), 2.10 (s, 3H arene-CH₃), 1.62–1.68 (m, 2H, arene-CH₂CH₂), 1.26 (d, ³J_{HH} = 6.7 Hz, 3H, CH₃). ³¹P NMR (CDCl₃): δ 24.6 (s, PPh₃). ESI-MS (acetone) *m/z* = 606.9 [Ru(η⁶-4-phenyl-2-butanol)Cl₂(PPh₃)]Na⁺ (100%), *m/z* = 549.2 [Ru(η⁶-4-phenyl-2-butanol)Cl(PPh₃)]⁺ (74%).

[Ru(η⁶-*p*-cymene)Cl₂(P(*p*-C₆H₄F)₃)] **8a**. [Ru(η⁶-*p*-cymene)Cl₂]₂ (150 mg, 0.22 mmol) and P(C₆H₄F)₃ (150 mg, 0.44 mmol) were refluxed in chloroform for 8 h at 70 °C. Yield; 266 mg (94%), red powder. Slow diffusion of diethyl ether into a dichloromethane solution gave crystals suitable for X-ray diffraction.

¹H NMR (CDCl₃): δ 7.82–7.80 (m, 6H, P(C₆H₄F)₃), 7.08–7.19 (m, 6H, P(C₆H₄F)₃), 5.27, (d, ³J_{HH} = 6.0 Hz, 2H, H_m) 5.00 (d, ³J_{HH} = 5.8 Hz, 2H, H_o), 2.86–2.95 (m, 1H, ¹Pr), 1.88 (s, 3H arene-CH₃), 1.16 (d, ³J_{HH} = 7.2 Hz, 6H, CH(CH₃)₂). ³¹P NMR (CDCl₃): δ 23.0 (s, P(C₆H₄F)₃). ESI-MS (acetone) *m/z* = 645.4 [Ru(η⁶-*p*-cymene)Cl₂(P(C₆H₄F)₃)]Na⁺ (100%), *m/z* = 587.1 [Ru(η⁶-*p*-cymene)Cl(P(C₆H₄F)₃)]⁺ (80%).

[Ru(η⁶-4-phenyl-2-butanol)Cl₂(P(C₆H₄F)₃)] **9a**. [Ru(η⁶-4-phenyl-2-butanol)Cl₂]₂ (100 mg, 0.16 mmol) and P(C₆H₄F)₃ (100 mg, 0.32 mmol). Yield; 174 mg (73%), red powder.

¹H NMR (CDCl₃): δ 7.52–7.58 (m, 6H, P(C₆H₄F)₃), 7.07–7.24 (m, 6H, P(C₆H₄F)₃), 5.68 (d, ³J_{HH} = 6.4 Hz, 2H, H_m), 5.24 (d, ³J_{HH} = 5.9 Hz, 2H, H_o) 4.68–4.72 (m, 1H, H_p), 2.76–2.82 (m, 1H, HCOH), 2.63 (s, 3H arene-CH₃), 1.80–1.85 (m, 2H, arene-CH₂CH₂), 1.26 (d, ³J_{HH} = 6.7 Hz, 3H, CH₃). ³¹P NMR (CDCl₃): δ 24.6 (s, P(C₆H₄F)₃). ESI-MS (acetone) *m/z* = 660.9 [Ru(η⁶-4-phenyl-2-butanol)Cl₂(P(C₆H₄F)₃)]Na⁺ (100%), *m/z* = 602.9 [Ru(η⁶-4-phenyl-2-butanol)Cl(P(C₆H₄F)₃)]⁺ (60%).

Compounds **1b–5b** and **8b–9b** were prepared according to the procedure described for **1b**.

[Ru(η⁶-*p*-cymene)(pta)Cl(PPh₂(*p*-C₆H₄C₂H₄C₈F₁₇))]BF₄ **1b**. To a methanol solution (20 mL) of **1a** (120 mg, 0.12 mmol) was added NH₄BF₄ (64 mg, 0.61 mmol), and the solution stirred for 1 h, after which a methanol solution of pta (21 mg, 0.13 mmol) in 10 mL was added dropwise over 30 min and stirred for a further 2 h. The solvent volume was reduced in vacuo to about 10 mL and product precipitated with hexane (10 mL). The resulting yellow powder was filtered and washed with hexane (2 × 20 mL). The resulting yellow powder was recrystallized from fluorobenzene and hexane. Yield; 123 mg (83%).

¹H NMR (CDCl₃): δ 7.55–7.67 (m, 6H, PPh₂Ar), 7.39–7.41 (m, 8H, PPh₂Ar), 6.46 (d, ³J_{HH} = 6.0 Hz, 1H, H_m), 5.89, (d, ³J_{HH} = 5.8 Hz, 1H, H_o), 5.76 (d, ³J_{HH} = 6.2 Hz, 1H, H_o), 5.12 (d, ³J_{HH} = 5.6 Hz, 1H, H_m), 4.45 (d, ²J_{HH} = 14.2 Hz, 3H, pta), 4.37 (d, ²J_{HH} = 15.0 Hz, 3H, pta), 4.28 (d, ²J_{HH} = 14.8 Hz, 3H, pta), 3.90 (d, ²J_{HH} = 14.6 Hz, 3H, pta), 3.00 (t, ³J_{HH} = 5.6 Hz, 4H, PhCH₂CH₂C₈F₁₇), 2.80–2.87 (m, 1H, ¹Pr), 2.41–2.45 (m, 2H, PhCH₂CH₂C₈F₁₇), 1.63 (s, 3H, arene-CH₃), 1.30 (d, ³J_{HH} = 7.0 Hz, 3H, CH(CH₃)₂), 1.28 (d, ³J_{HH} = 6.6 Hz, 3H, CH(CH₃)₂). ³¹P NMR (CDCl₃): δ 30.0 (d, ²J_{PP} = 52 Hz, PPh₂Ar), –42.7 (d, ²J_{PP} = 54 Hz, pta). ESI-MS (MeOH) *m/z* = 1136.2 [Ru(η⁶-*p*-cymene)(pta)Cl(PPh₂(Ph(C₂H₄C₈F₁₇)))]⁺ (100%). *T*_{decomp} 160 °C.

[Ru(η⁶-*p*-cymene)(pta)Cl(PPh(*p*-C₆H₄C₂H₄C₈F₁₇))₂]BF₄ **2b**. **5a** (180 mg, 0.12 mmol), NH₄BF₄ (63 mg, 0.60 mmol) and pta (21 mg, 0.13 mmol) in 10 mL. Yield; 156 mg (80%) of yellow powder.

¹H NMR (CDCl₃): δ 7.59–7.69 (m, 6H, PPhAr₂), 7.3–7.41 (m, 7H, PPhAr₂), 6.66 (d, ³J_{HH} = 6.0 Hz, 1H, H_o), 6.02 (d, ³J_{HH} = 6.8 Hz, 1H, H_m), 5.78 (d, ³J_{HH} = 5.6 Hz, 1H, H_m), 5.05

(d, $^3J_{\text{HH}} = 5.8$ Hz, 1H, H_m), 4.41 (d, $^2J_{\text{HH}} = 12$ Hz, 3H, *pta*), 4.26 (d, $^2J_{\text{HH}} = 12$ Hz, 3H, *pta*), 4.16 (d, $^2J_{\text{HH}} = 16$ Hz, 3H, *pta*), 3.89 (d, $^2J_{\text{HH}} = 16$ Hz, 3H, *pta*), 3.01 (t, $^3J_{\text{HH}} = 6.2$ Hz, 4H, PhCH₂CH₂C₆F₁₇), 2.73–2.79 (m, 1H, ¹Pr), 2.41–2.43 (m, 4H, PhCH₂CH₂C₆F₁₇), 1.65 (s, 3H arene-CH₃), 1.32 (d, $^3J_{\text{HH}} = 6.8$ Hz, 3H, CH(CH₃)₂), 1.30 (d, $^3J_{\text{HH}} = 7.0$ Hz, 3H, CH(CH₃)₂). ³¹P NMR (CDCl₃): δ 29.7 (d, $^2J_{\text{PP}} = 55$ Hz, PPhAr₂), −43.1 (d, $^2J_{\text{PP}} = 55$ Hz, *pta*). ESI-MS (MeOH) *m/z* = 1588.1 [Ru(η⁶-*p*-cymene)(*pta*)Cl(PPh(*p*-C₆H₄C₂H₄C₈F₁₇)₂)] (100%). mp 167–170 °C.

[Ru(η⁶-*p*-cymene)(*pta*)Cl(P(*p*-C₆H₄C₂H₄C₆F₁₃)₃)BF₄ **3b**. **3a** (200 mg, 0.12 mmol), NH₄BF₄ (64 mg, 0.61 mmol), and *pta* (20 mg, 0.12 mmol in 10 mL). Yield; 171 mg (79%) of yellow powder.

¹H NMR (CDCl₃): δ 7.56–7.60 (m, 6H, PAr₃), 7.39–7.41 (m, 6H, PAr₃), 6.68 (d, $^3J_{\text{HH}} = 5.6$ Hz, 1H, H_o), 6.04, (d, $^3J_{\text{HH}} = 5.8$ Hz, 1H, H_m), 5.76 (d, $^3J_{\text{HH}} = 6.0$ Hz, 1H, H_m), 5.03 (d, $^3J_{\text{HH}} = 5.6$ Hz, 1H, H_o), 4.44 (d, $^2J_{\text{HH}} = 13.8$ Hz, 3H, *pta*), 4.36 (d, $^2J_{\text{HH}} = 14.2$ Hz, 3H, *pta*), 4.07 (d, $^2J_{\text{HH}} = 12.0$ Hz, 3H, *pta*), 3.90 (d, $^2J_{\text{HH}} = 10.2$ Hz, 3H, *pta*), 3.00 (t, $^3J_{\text{HH}} = 5.8$ Hz, 6H, PhCH₂CH₂C₆F₁₃), 2.78–2.86 (m, 1H, ¹Pr), 2.43–2.44 (m, 6H, PhCH₂CH₂C₆F₁₃), 1.63 (s, 3H arene-CH₃), 1.30 (d, $^3J_{\text{HH}} = 6.8$ Hz, 3H, CH(CH₃)₂), 1.28 (d, $^3J_{\text{HH}} = 6.2$ Hz, 3H, CH(CH₃)₂). ³¹P NMR (CDCl₃): δ 29.8 (d, $^2J_{\text{PP}} = 55$ Hz 1P, PAr₃), −43.3 (d, $^2J_{\text{PP}} = 55$ Hz, *pta*). ESI-MS (MeOH) *m/z* = 1727.2 [Ru(η⁶-*p*-cymene)Cl₂(P(*p*-C₆H₄C₆F₁₃)₃)] (100%). mp 172–177 °C.

[Ru(η⁶-4-phenyl-2-butanol)(*pta*)Cl(PPh₂(*p*-C₆H₄C₂H₄C₈F₁₇))]-BF₄ **4b**. **4a** (120 mg, 0.11 mmol), NH₄BF₄ (64 mg, 0.61 mmol) and *pta* (17 mg, 0.11 mmol in 10 mL). The product was isolated as a racemic mixture. Yield; 102 mg (75%) of yellow powder.

¹H NMR (CDCl₃): δ 7.55–7.74 (m, 6H, PPh₂Ar), 7.43–7.50 (m, 8H, PPh₂Ar), 6.74 (d, $^3J_{\text{HH}} = 5.6$ Hz, 1H, H_o), 6.22, (d, $^3J_{\text{HH}} = 4.8$ Hz, 1H, H_m), 5.69 (d, $^3J_{\text{HH}} = 5.4$ Hz, 1H, H_m), 5.28 (d, $^3J_{\text{HH}} = 5.8$ Hz, 1H, H_o), 4.71 (d, $^2J_{\text{HH}} = 12.6$ Hz, 3H, *pta*), 4.62–4.65 (m, 1H, H_p), 4.39 (d, $^2J_{\text{HH}} = 14.8$ Hz, 3H, *pta*), 4.23 (d, $^2J_{\text{HH}} = 14.2$ Hz, 3H, *pta*), 3.90 (d, $^2J_{\text{HH}} = 10.6$ Hz, 3H, *pta*), 3.01 (t, $^3J_{\text{HH}} = 6.2$ Hz, 2H, PhCH₂CH₂C₈F₁₇), 2.73–2.78 (m, 1H, HCOH), 2.46–2.50 (m, 2H, PhCH₂CH₂C₈F₁₇), 1.63 (s, 3H arene-CH₃), 1.76–1.79 (m, 2H, arene-CH₂CH₂), 1.27 (d, $^3J_{\text{HH}} = 7.0$ Hz, 3H, CH₃). ³¹P NMR (CDCl₃): δ 31.4 (d, $^2J_{\text{PP}} = 54$ Hz, PPh₂Ar), 31.3 (d, $^2J_{\text{PP}} = 54$ Hz, PPh₂Ar), −40.4 (d, $^2J_{\text{PP}} = 55$ Hz, *pta*), −40.5 (d, $^2J_{\text{PP}} = 55$ Hz, *pta*).^a ESI-MS (MeOH) *m/z* = 1152.2 [Ru(η⁶-phenyl-butanol)(*pta*)Cl(PPh₂(Ph(C₂H₄C₈F₁₇)))⁺ (100%). *T*_{decomp.} 157 °C.

[Ru(η⁶-4-phenyl-2-butanol)(*pta*)Cl(PPh(*p*-C₆H₄C₂H₄C₈F₁₇)₂)]-BF₄ **5b**. **5a** (90 mg, 0.07 mmol), NH₄BF₄ (37 mg, 0.35 mmol) and *pta* (12 mg, 0.8 mmol in 10 mL). The product was isolated as a racemic mixture. Yield; 91 mg (90%) of yellow powder.

¹H NMR (CDCl₃): δ 7.55–7.74 (m, 6H, PPhAr₂), 7.43–7.50 (m, 7H, PPhAr₂), 6.67 (d, $^3J_{\text{HH}} = 5.6$ Hz, 1H, H_o), 6.13, (d, $^3J_{\text{HH}} = 6.0$ Hz, 1H, H_m), 5.65 (d, $^3J_{\text{HH}} = 6.2$ Hz, 1H, H_m), 5.30 (d, $^3J_{\text{HH}} = 5.8$ Hz, 1H, H_o), 4.73 (d, $^2J_{\text{HH}} = 12.0$ Hz, 3H, *pta*), 4.45–4.51 (m, 1H, H_p), 4.23 (d, $^2J_{\text{HH}} = 13.2$ Hz, 3H, *pta*), 4.10 (d, $^2J_{\text{HH}} = 13.6$ Hz, 3H, *pta*), 3.90 (d, $^2J_{\text{HH}} = 14.0$ Hz, 3H, *pta*), 3.02 (t, $^3J_{\text{HH}} = 6.0$ Hz, 4H, PhCH₂CH₂C₈F₁₇), 2.81–2.84 (m, 1H, HCOH), 2.41–2.45 (m, 4H, PhCH₂CH₂C₈F₁₇), 1.96–1.20 (m, 2H arene-CH₂CH₂), 1.81–1.85 (m, 2H, arene-CH₂CH₂), 1.27 (d, $^3J_{\text{HH}} = 7.0$ Hz, 3H, CH₃). ³¹P NMR (CDCl₃): δ 30.9 (d, $^2J_{\text{PP}} = 54$ Hz, PPhAr₂), 30.8 (d, $^2J_{\text{PP}} = 53$ Hz, PPhAr₂), −41.4 (d, $^2J_{\text{PP}} = 54$ Hz, *pta*), −41.5 (d, $^2J_{\text{PP}} = 54$ Hz, *pta*). [Two Ru,C configurational diastereomers are present at equal ratio] ESI-MS (MeOH) *m/z* = 1594.1 [Ru(η⁶-phenyl-butanol)(*pta*)Cl(PPh(*p*-C₆H₄C₂H₄C₈F₁₇)₂)]⁺ (100%), *m/z* = 1444.9 [Ru(*pta*)Cl(PPh(*p*-C₆H₄C₂H₄C₈F₁₇)₂)]⁺ (40%). *T*_{decomp.} 144 °C.

[Ru(η⁶-*p*-cymene)(*pta*)Cl(P(C₆H₄F₃))BF₄ **8b**. **8a** (222 mg, 0.31 mmol), NH₄BF₄ (164 mg, 1.56 mmol) and *pta* (50 mg, 0.32 mmol in 10 mL). Yield; 101 mg (93%) of yellow powder.

¹H NMR (CDCl₃): δ 7.52–7.595 (m, 6H, P(C₆H₄F₃)), 7.04–7.19 (m, 6H, P(C₆H₄F₃)), 6.58 (d, $^3J_{\text{HH}} = 6.0$ Hz, H, H_m),

5.94 (d, $^3J_{\text{HH}} = 5.7$ Hz, 1H, H_o), 5.76 (d, $^3J_{\text{HH}} = 6.2$ Hz, 1H, H_o), 5.14 (d, $^3J_{\text{HH}} = 5.8$ Hz, 1H, H_m), 4.70 (d, $^2J_{\text{HH}} = 12.0$ Hz, 3H, *pta*), 4.33 (d, $^2J_{\text{HH}} = 12.8$ Hz, 3H, *pta*), 4.20 (d, $^2J_{\text{HH}} = 13.8$ Hz, 3H, *pta*), 3.81 (d, $^2J_{\text{HH}} = 12.4$ Hz, 3H, *pta*), 2.60–2.67 (m, 1H, ¹Pr), 1.24 (d, $^3J_{\text{HH}} = 6.5$ Hz, 3H, CH(CH₃)₂), 1.22 (d, $^3J_{\text{HH}} = 6.8$ Hz, 3H, CH(CH₃)₂). ³¹P NMR (CDCl₃): δ 28.8 (d, $^2J_{\text{PP}} = 54$ Hz, P(C₆H₄F₃)), −42.5 (d, $^2J_{\text{PP}} = 54$ Hz, *pta*). ESI-MS (MeOH) *m/z* = 744.1 [Ru(η⁶-*p*-cymene)(*pta*)Cl(P(C₆H₄F₃))] (100%). *T*_{decomp.} 250 °C.

[Ru(η⁶-4-phenyl-2-butanol)(*pta*)Cl(P(C₆H₄F₃))BF₄ **9b**. **9a** (69 mg, 0.66 mmol), NH₄BF₄ (64 mg, 0.61 mmol) and *pta* (22 mg, 0.15 mmol in 10 mL). The product was isolated as a racemic mixture. Yield; 101 mg (93%) of yellow powder.

¹H NMR (CDCl₃): δ 7.54–7.59 (m, 6H, P(C₆H₄F₃)), 7.07–7.24 (m, 6H, P(C₆H₄F₃)), 6.86 (d, $^3J_{\text{HH}} = 5.8$ Hz, 1H, H_o), 6.19, (d, $^3J_{\text{HH}} = 6.1$ Hz, 1H, H_m), 5.68 (d, $^3J_{\text{HH}} = 5.8$ Hz, 1H, H_m), 5.15 (d, $^3J_{\text{HH}} = 6.2$ Hz, 1H, H_o), 4.71 (d, $^2J_{\text{HH}} = 12.4$ Hz, 3H, *pta*), 4.60–4.64 (m, 1H, H_p), 4.39 (d, $^2J_{\text{HH}} = 13.5$ Hz, 3H, *pta*), 4.23 (d, $^2J_{\text{HH}} = 13.2$ Hz, 3H, *pta*), 3.90 (d, $^2J_{\text{HH}} = 12.8$ Hz, 3H, *pta*), 2.79–2.83 (m, 1H, HCOH), 2.63 (s, 3H arene-CH₃), 1.79–1.82 (m, 2H, arene-CH₂CH₂), 1.26 (d, $^3J_{\text{HH}} = 6.5$ Hz, 3H, CH₃). ³¹P NMR (CDCl₃): δ 30.5 (d, $^2J_{\text{PP}} = 53$ Hz, P(C₆H₄F₃)), 30.3 (d, $^2J_{\text{PP}} = 54$ Hz, P(C₆H₄F₃)), −41.0 (d, $^2J_{\text{PP}} = 54$ Hz, *pta*), −41.2 (d, $^2J_{\text{PP}} = 54$ Hz, *pta*).^a ESI-MS (MeOH) *m/z* = 759.1 [Ru(η⁶-phenyl-butanol)(*pta*)Cl(P(C₆H₄F₃))] (100%). *T*_{decomp.} 162 °C.

[Ru(η⁶-4-phenyl-2-butanol)(*pta*)Cl(P(*p*-C₆H₄C₂H₄C₆F₁₃))]-BF₄ **6b**. [Ru(η⁶-4-phenyl-2-butanol)(*pta*)Cl₂] (144 mg, 0.3 mmol) was refluxed in acetonitrile with 2 mol equiv of NH₄BF₄ for 1 h. The solution was filtered, and the solvent removed at reduced pressure. The resulting solids were extracted with methanol and precipitated with diethyl ether. The yellow powder was stirred for 2 days with an excess of P(*p*-C₆H₄C₂H₄C₆F₁₃)₃ (780 mg, 0.6 mmol) in methanol following which the solution was filtered to remove unreacted P(*p*-C₆H₄C₂H₄C₆F₁₃)₃, the solvent volume reduced, and the product precipitated with hexane as a yellow solid. The product was isolated as a racemic mixture. Yield; 122 mg (67%).

¹H NMR (d⁶-DMSO): δ 7.41–7.62 (m, 6H, PAr₃), 6.91–7.10 (m, 6H, PAr₃), 6.58 (d, $^3J_{\text{HH}} = 5.5$ Hz, 1H, H_o), 6.13, (d, $^3J_{\text{HH}} = 6.0$ Hz, 1H, H_m), 5.65 (d, $^3J_{\text{HH}} = 5.8$ Hz, 1H, H_m), 5.22 (d, $^3J_{\text{HH}} = 5.6$ Hz, 1H, H_o), 4.73 (d, $^2J_{\text{HH}} = 12.0$ Hz, 3H, *pta*), 4.58–4.62 (m, 1H, H_p), 4.23 (d, $^2J_{\text{HH}} = 12.3$ Hz, 3H, *pta*), 4.10 (d, $^2J_{\text{HH}} = 12.8$ Hz, 3H, *pta*), 3.90 (d, $^2J_{\text{HH}} = 13.2$ Hz, 3H, *pta*), 3.00–3.04 (m, 6H, PhCH₂CH₂C₆F₁₃), 2.82–2.85 (m, 1H, HCOH), 2.43–2.46 (m, 6H, PhCH₂CH₂C₆F₁₃), 1.99–2.02 (m, 2H arene-CH₂CH₂), 1.84 (m, 2H, arene-CH₂CH₂), 1.27 (d, $^3J_{\text{HH}} = 6.8$ Hz, 3H, CH₃). ³¹P NMR (d⁶-DMSO): δ 29.4 (d, $^2J_{\text{PP}} = 54$ Hz, PAr₃), 29.2 (d, $^2J_{\text{PP}} = 54$ Hz, PAr₃), −42.0 (d, $^2J_{\text{PP}} = 55$ Hz, *pta*), −42.2 (d, $^2J_{\text{PP}} = 55$ Hz, *pta*).^a ESI-MS (MeOH) *m/z* = 1744.2 [Ru(η⁶-phenyl-butanol)(*pta*)Cl(P(*p*-C₆H₄C₆F₁₃))]⁺ (100%). *T*_{decomp.} 137 °C.

[Ru(η⁶-4-phenyl-2-butanol)(*pta*)Cl(PPh₃)]BF₄ **7b**. [Ru(η⁶-4-phenyl-2-butanol)(*pta*)Cl₂] (80 mg, 0.17 mmol), NH₄BF₄ (90 mg, 0.86 mmol), followed by triphenylphosphine (50 mg, 0.19 mmol). The solution was stirred at room temperature for 5 h, the solvent volume reduced, and hexane added to induce precipitation. The resulting yellow solid was washed with hexane (2 × 20 mL) and diethyl ether (2 × 20 mL). Yield; 123 mg (91%).

¹H NMR (CDCl₃): δ 7.59–7.68 (m, 6H, PPh₃), 7.30–7.35 (m, 9H, PPh₃), 6.66 (d, $^3J_{\text{HH}} = 5.8$ Hz, 2, H_o), 6.13, (d, $^3J_{\text{HH}} = 6.2$ Hz, H, H_m), 5.71 (d, $^3J_{\text{HH}} = 5.5$ Hz, 1H, H_m), 5.40 (d, $^3J_{\text{HH}} = 6.0$ Hz, 1H, H_o), 4.69 (d, $^2J_{\text{HH}} = 12.8$ Hz, 3H, *pta*), 4.62 (d, $^2J_{\text{HH}} = 15.5$ Hz, 3H, *pta*), 4.56–4.60 (m, 1H, H_p), 4.24 (d, $^2J_{\text{HH}} = 14.8$ Hz, 3H, *pta*), 3.92 (d, $^2J_{\text{HH}} = 13.0$ Hz, 3H, *pta*), 2.78–2.82 (m, 1H, HCOH), 1.78–1.81 (m, 2H arene-CH₂CH₂), 1.68 (m, 2H, arene-CH₂CH₂), 1.26 (d, $^3J_{\text{HH}} = 6.8$ Hz, 3H, CH₃). ³¹P NMR (CDCl₃): δ 30.5 (d, $^2J_{\text{PP}} = 53$ Hz, PPh₃), 30.4 (d,

Table 4. Solubility of **1b**, **4b**, **5b**, **7b**, and **9b** in H₂O

	<i>S</i> (mM) 20 °C	<i>S</i> (mM) 30 °C	<i>S</i> (mM) 37 °C	<i>S</i> (mM) 40 °C	<i>S</i> (mM) 42 °C	<i>S</i> (mM) 45 °C
1b	0	0	0.1	0.2	0.3	0.7
4b	2.6	11	19	23	26	31
5b	0	0	0.1	0.1	0.3	0.4
7b	3.9	3.9	5.0	5.4	5.6	6.1
9b	5.1	5.1	5.3	5.3	5.3	5.4

²*J*_{PP} = 53 Hz, *PPh*₃), −42.5 (d, ²*J*_{PP} = 54 Hz, *pta*), −42.7 (d, ²*J*_{PP} = 54 Hz, *pta*).^a *T*_{decomp.} 180 °C.

Hydrolysis Study. A 1 mM solution of **4b** in D₂O was incubated over 3 days at 37 °C. Aliquots were taken after 1, 2, 5, 24, 48, 72, and 168 h and analyzed by ³¹P NMR spectroscopy.

Solubility Measurements. Samples of a known mass were suspended in H₂O (2 mL) and incubated for 30 min at temperatures ranging between 20 and 45 °C. The sample was filtered to remove any insoluble material, and 990 μL transferred to an NMR tube containing 10 μL of a known concentration of triethylphosphate. The concentration of compound in solution was determined by integration of the ³¹P NMR spectra to give the ratio of compound to triethylphosphate. The mass of the sample in the initial suspension and the volume of triethylphosphate were adjusted according to the solubility of the compound. For example, for **1b** at 20 °C 0.8 mmol (2 mg of a 20 mg/20 mL solution) of the complex with 11 mmol (10 μL from a 1:9 v/v solution of triethylphosphate/H₂O) of triethylphosphate, for **4b** at 20 °C 10 mmol (25 mg/2 mL) of the complex with 22 mmol (10 μL from a 2:8 v/v solution of triethylphosphate/H₂O) of triethyl phosphate. Concentrations at each temperature measured are given in Table 4.

X-ray Structure Determination. Data for **8b** was collected on a KUMA CCD diffractometer system using graphite-monochromated Mo Kα radiation. Data reduction was performed with CrysAlis RED.³⁹ The structure was solved by direct methods with SHELXS-97⁴⁰ and refined by least-squares fit on *F*² using SHELXL-97.⁴⁰ The absorption correction was applied using the multiscan procedure SADABS.⁴¹ All non-hydrogen atoms were refined anisotropically with hydrogen atoms placed in geometrically calculated positions and refined using a riding model. ORTEP³⁴² was used to produce the graphical representation of **8b**. Relevant data is given in Table 5.

Cell Line and Culture Conditions. The human A2780 ovarian cancer cell line was obtained from the European Collection of Cell Cultures (Salisbury, U.K.). Cells were grown routinely in RPMI medium containing glucose, 5% fetal calf serum (FCS), and antibiotics at 37 °C and 5% CO₂.

Cytotoxicity Test (MTT Assay). Cytotoxicity was determined using the MTT assay (MTT = 3-(4,5-dimethyl-2-thiazolyl)-2,5-diphenyl-2*H*-tetrazolium bromide). Cells were seeded in 96-well

Table 5. Selected Crystallographic Data for **8b**

parameter	8b
formula	C ₃₄ H ₃₈ BClF ₇ N ₃ P ₂ Ru
fw (g mol ^{−1})	830.94
crystal system	monoclinic
space group	<i>P</i> 2 ₁ / <i>c</i>
<i>a</i> (Å)	14.4292(3)
<i>b</i> (Å)	14.2971(3)
<i>c</i> (Å)	17.6308(4)
α (deg)	90
β (deg)	109.367(2)
γ (deg)	90
volume (Å ³)	3431.35(12)
<i>Z</i>	4
<i>D</i> _{calc} (g cm ^{−3})	1.608
μ (mm ^{−1})	0.697
<i>F</i> (000)	1688
temp (K)	140(2)
measured reflns	22576
unique reflns	6949
θ range (deg)/completeness (%)	2.99 to 26.37/99.1
no. of data/parameters/restraints	6949/483/92
GoF ^a	1.039
<i>R</i> ^b [<i>I</i> > 2σ(<i>I</i>)]	0.0290
<i>wR</i> ^{2b} (all data)	0.0723
largest diff. peak/hole (e Å ^{−3})	1.566/−0.546

^a GoF is defined as $\{\sum[w(F_o^2 - F_c^2)^2]/(n - p)\}^{1/2}$ where *n* is the number of data and *p* is the number of parameters refined. ^b *R* = $\sum||F_o| - |F_c||/\sum|F_o|$, *wR*² = $\{\sum w(F_o^2 - F_c^2)^2/\sum w(F_o^2)\}^{1/2}$.

plates as monolayers with 100 μL of cell solution (approximately 20,000 cells) per well and preincubated for 24 h in medium supplemented with 10% FCS. With the exception of **4b** and **9b**, which were dissolved directly in the culture medium, compounds were added as DMSO solutions and serially diluted to the appropriate concentration (to give a final DMSO concentration of 0.5%). A 100 μL portion of drug solution was added to each well, and the plates were incubated for another 72 h. Subsequently, MTT (5 mg/mL solution in phosphate buffered saline) was added to the cells, and the plates were incubated for a further 2 h. The culture medium was aspirated, and the purple formazan crystals formed by the mitochondrial dehydrogenase activity of vital cells were dissolved in DMSO. The optical density, directly proportional to the number of surviving cells, was quantified at 540 nm using a multiwell plate reader (iEMS Reader MF, Labsystems, U.S.), and the fraction of surviving cells was calculated from the absorbance of untreated control cells. Evaluation is based on means from 2 independent experiments, each comprising 3 microcultures at each concentration level.

Acknowledgment. We thank the Swiss National Science Foundation and EPFL for financial support and Severine Moret for preparing **1a–3a**.

Supporting Information Available: The crystallographic information file (cif) of complex **8b**. This material is available free of charge via the Internet at <http://pubs.acs.org>.

(39) CrysAlis PRO; Oxford Diffraction Ltd.: Abingdon, Oxfordshire, U.K., 2009.

(40) Sheldrick, G. M. SHELX97; University of Göttingen: Göttingen, Germany, 1997.

(41) Sheldrick, G. M. SADABS, version 2006; University of Göttingen: Göttingen, Germany, 1997.

(42) Farrugia, L. J. *J. Appl. Crystallogr.* **1997**, *30*, 565.